VOL. 16, NO. 24, DECEMBER 2021 ISSN 1819-6608
ARPN Journal of Engineering and Applied Sciences

www.arpnjournals.com

AN EMPIRICAL STUDY ON THE EFFECTIVENESS OF ENERGY HARVESTING FROM DYNAMIC VIBRATION ABSORBER

Luqmaan Hakiem Sulaiman[1], M. Azhan Anuar[2] and Zamri A. R.[2]
[1]INTEKMA Sdn. Bhd., D17-03 and 03A, Menara Mitraland No, 13A, Jalan PJU 5/1, Pju 5 Kota Damansara, Petaling Jaya, Selangor, Malaysia
[2]School of Mechanical Engineering, College of Engineering, UniversitiTeknologi MARA, Shah Alam, Malaysia
E-Mail: azhan788@uitm.edu.my

ABSTRACT

Dynamic Vibration Absorber (DVA) consisting of a simple mass-stiffness mechanism has typically been designed to attenuate excessive vibrations in machines and structures operating at or near their resonant frequencies. This undamped DVA, namely the auxiliary system, helps to reduce the amplitude of the main system by creating the "anti-node" and theoretically lags 180º of the excitation force in order to suppress the vibration amplitude of the main system.DVA demonstrates unused and wasted energy that can potentially be harvested for other purposes. Energy harvesting from the vibration object, which in this case is the DVA, is a technique used to convert unwanted vibrations into electrical energy. This paper will address the effect of the DVA parameters chosen on the basis of the Randy Fox Method (RFM) and its effectiveness will be experimentally tested. The piezoelectric transducer is mounted on the DVA and the energy produced in the form of the generated voltage is measured at different widths of 30 mm, 40 mm and 50 mm for three different tuned mass positions. The experimental results reveal that a single piezoelectric transducer can generate up to 40 millivolts at an operating frequency that excites the original natural frequencies of the main system. It is observed that with the proper selection of parameters, the vibration amplitude of the main system is attenuated effectively along with the sufficient energy that can be harvested.

Keywords: dynamic absorber, energy harvesting, natural frequency, piezoelectric, resonance.

INTRODUCTION

Vibrations in machinery are a common problem faced throughout the industry. It may cause deterioration, hence shortening the lifetime of the machine and in some cases pose danger to people surrounding it. This problem is most significant for systems operating at a frequency which coincides at or in the neigbourhood of its own natural frequency.

The installation of a dynamic vibration absorber (DVA), which is made of a simple mass-stiffness system, has commonly been used to attenuate the vibration for a targeted range of frequency. This is one of the alternative techniques that has been developed to suppress the amplitude of the vibration of the main system. DVA can be designed and tested before installation. It can be adjusted in the lab environment with predictable field results[1].

Over the years, different types of DVA have been developed and implemented in a wide range of applications, such as passive type [2] and active types [3]. Designs and methodologies are centered on the applicability and suitability of the required DVA and have been successfully applied in rail structure [4], marine application [5], rotating machinery [6]and also in civil structures [7], [8]. The difference between the two types of DVA is that passive type uses fixed stiffness and damping while active type adds force generator. The active and passive concepts used interchangeably in suspension for the automotive industry. They have been implemented in many different ways [9].

In practice, the natural frequency of the DVA must be tuned to ensure that it is similar or close to the frequency of the excitation to the main system, which make determination of the natural frequency of the main system becomes important. For this, experimental method such as Operational Modal Analysis (OMA), is commonly used to determine the dynamic characteristics of the main system [10]. The OMA method was successfully performed to assist in areliable determination of the required parameters for DVA when designing the DVA for a main system with no dynamic characteristic information. It is even ascertained that when the excitation frequency is near or similar to the natural frequency of the main system, the dynamic absorber works effectively[11].

In order to have sufficient strength to absorb the energy of a main system, an effective DVA must be designed with the correct mass and stiffeness ratio [12]. Theoretically, it is understood that the mass of the DVA needs to be sufficiently large to ensure a wider natural frequency distance in the combined system. However, this is extremely impractical in certain cases and the application really depends a lot on the specification and suitability. Since the selection of the tune mass and its position is typically carried out by experienced designers/engineers, the use of the design template to assist new designers/engineers to build DVA is made available [13].

While the DVA might have solved the major problem of the excessively vibrating system, the vibration of the DVA is simply let to waste. This situation hints at a potential for energy harvesting by using piezoelectric transducers. Research on the DVA and piezoelectric transducers are very common individually, but the combination of both is less reported [14].

Attaching a piezoelectric transducer on a vibrating host structure will induce electricity since

piezoelectric materials produce electricity when it experiences strain. Researchers are currently developing energy harvesting solutions for continuous, independent power supply for the system to operate using piezoelectric application [15]-[17].

In this study, the design of the DVA is performed from the analytical derivation using Randy Fox equation and subsequently verified with the Graphical User Interface (GUI) templates that has been constructed [13]. Based on the Randy Fox formulation, effective parameters to fabricate the DVA are determined. The performance of the DVA to suppress the amplitude in the main system is determined by the measured displacement and its energy harvesting efficiency is measured by the generated voltage. The effectiveness of energy harvesting using piezoelectric transducer attached to the DVA with different parameters designed is compared. The voltage produced is limited to only one identical piezoelectric tranducer attached to a single DVA of the same material, thickness and length.

THEORETICAL BACKGROUND

Dynamic Vibration Absorber (DVA)

The purpose of DVA which consist of an auxiliary system of mass, M_2 and stiffness, k_2 attached to the main system, $M_1$is to reduce or eliminate unwanted vibration in the main system. This will result in a two degree of freedom system, consisting of as shown in Figure-1 and Figure-2.

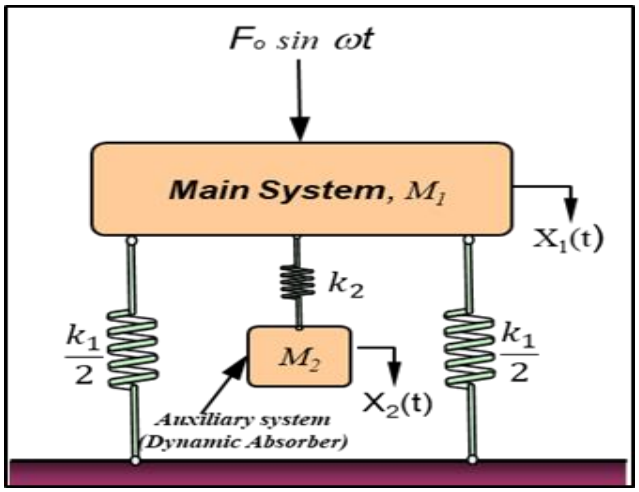

Figure-1. Auxiliary system as a dynamic absorber system.

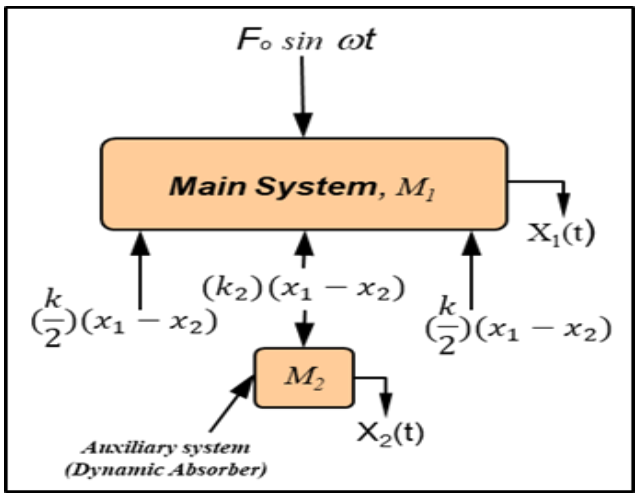

Figure-2. Free body diagram of undamped dynamic absorber system.

The equations of motion of masses based on free-body diagram (FBD) can be grouped into:
For main system,

$$+\downarrow \sum F_{x1} = m_1 \ddot{x}_1 \quad (1)$$

$$F_0 \sin \omega t - 2\left(k_1/2\right) - k_2(x_1 - x_2) = m_1 \ddot{x}_1$$

$$m_1 \ddot{x}_1 + 2\left(k_1/2\right) + k_2(x_1 - x_2) = F_0 \sin \omega t$$

For auxiliary system,

$$+\downarrow \sum F_{x2} = m_2 \ddot{x}_2 \quad (2)$$

$$k_2(x_1 - x_2) = m_2 \ddot{x}_2$$

$$m_1 \ddot{x}_1 + k_2(x_2 - x_1) = 0$$

Assuming harmonic solution in the following form,

$$x_1 = X_1 \sin \omega t \quad (3.a)$$

$$x_2 = X_2 \sin \omega t \quad (3.b)$$

The substitution of the solution yields the steady-state amplitude for masses 1 and 2 as the following,

$$X_1 = \frac{(k_2 - m_2\omega^2)F_0}{(k_1 + k_2 - m_1\omega^2)(k_2 - m_2\omega^2) - {k_2}^2} \quad (4.a)$$

$$X_2 = \frac{k_2 F_0}{(k_1 + k_2 - m_1\omega^2)(k_2 - m_2\omega^2) - {k_2}^2} \quad (4.b)$$

Since the purpose of the DVA is to reduce the amplitude of the main system, X_1, the numerator of X_1 is set to be equal to zero which gives

$$\omega^2 = \frac{k_2}{m_2} \quad (5)$$

This is also in the condition that the main system is originally operating near its resonance, where $\omega^2 \cong {\omega_1}^2 = k_1/m_1$. By letting

$$\omega^2 = \frac{k_2}{m_2} = \frac{k_1}{m_1} \quad (6)$$

the amplitude of vibration of the main system will be zero when operating at its original resonant frequency. Using the definition

$$\delta_{st} = \frac{F_0}{k_1}, \quad \omega_1 = \sqrt{\frac{k_1}{m_1}}, \quad \omega_2 = \sqrt{\frac{k_2}{m_2}} \quad (7)$$

where $\omega_1$and ω_2 are the natural frequencies of the main and auxiliary (DVA) systems, respectively. Equations (4.a) and (4.b) can be written as

$$\frac{X_1}{\delta_{st}} = \frac{1-\left(\frac{\omega}{\omega_2}\right)^2}{\left[1+\frac{k_2}{k_1}-\left(\frac{\omega}{\omega_1}\right)^2\right]\left[1-\left(\frac{\omega}{\omega_2}\right)^2\right]-\frac{k_2}{k_1}} \quad (8.a)$$

$$\frac{X_2}{\delta_{st}} = \frac{1}{\left[1+\frac{k_2}{k_1}-\left(\frac{\omega}{\omega_1}\right)^2\right]\left[1-\left(\frac{\omega}{\omega_2}\right)^2\right]-\frac{k_2}{k_1}} \quad (8.b)$$

$$X_2 = -\frac{k_1}{k_2}\delta_{st} = -\frac{F_0}{k_2} \quad (9)$$

From equation (9), it can be seen that X_1 is reduced to zero by the opposite impression force, i.e.

$$k_2 X_2 = m_2 \omega^2 X_2 = -F_0 \quad (10)$$

Piezoelectric Transducer

Piezoelectricity is a phenomenon where a particular material demonstrates an electromechanical coupling between their thermal, mechanical and electrical states with applied mechanical stress [18]. Piezoelectric materials may have direct effects when the material experiences mechanical stress or strain or converse effects when electrical field is applied which causes mechanical stress or strain. The electrical charge will be produced when there is mechanical stress or strain in piezoelectric materials. The schematic of piezoelectric effect is shown in Figure-3.

The electricity produced by piezoelectric materials under cyclic strain is in the AC form, which corresponds to the source of strain.

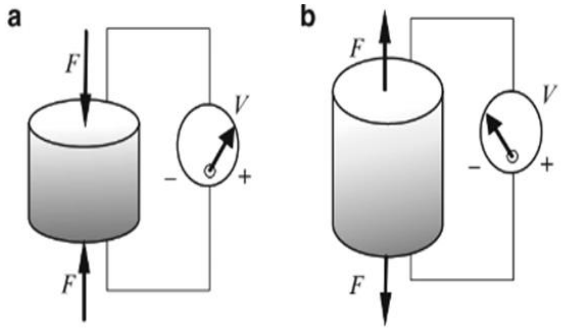

Figure-3. Schematic of piezoelectric effect in axial configuration [18].

For energy harvesting purpose, for example, a piezoelectric transducer can be attached to a cantilever DVA in order to utilise the bending and for adjustable resonance of the absorber as depicted in Figure-4.

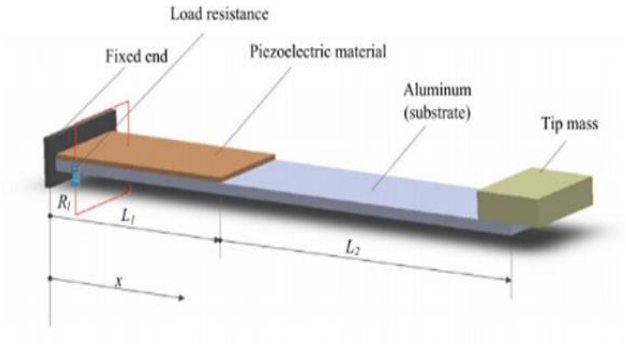

Figure-4. Schematic diagram of cantilever vibration absorber with piezoelectric material attachment [19].

Randy Fox Equation (RFM)

For RFM method, the analytical derivation for tune mass (M_2) is taken directly from RFM derivation[20]. The amount of this tune mass is given by

$$M_2 = \frac{(2.115\times10^5)EI}{{N_f}^2(3a^2L-a^3)} - \frac{0.75M_1L^4}{3a^2L-a^3} \quad (11)$$

Equation (11) indicates the amount of tune mass (M_2) needed at a specified distance, a on a piece of flat or rectangular bar stock of length L, having cross-sectional dimensions of$b$ and h to achieve the desired natural frequency N_f.

METHODOLOGY AND EXPERIMENTAL SETUP

Parameter Selection

The parameters for the dynamic absorber design to be used were determined with the aid of GUI developed using Randy-Fox Method as it was found to have better performance as compared to that of Dunkerley method [13], as illustrated in Figure-5. Material used for all dynamic absorbers was 1 mm thick aluminium due to availability and through calculations; it was recommended

that the total mass of the dynamic absorber including additional mass would not exceed 10% of that of the main system in accordance to the rule of thumb for dynamic absorber design. Additionally, the length of the dynamic absorber was set to 0.2302 m (i.e. a value given by the GUI template) which results in a reasonable range of tune mass to be added while still maintain within 10% of the original total mass.

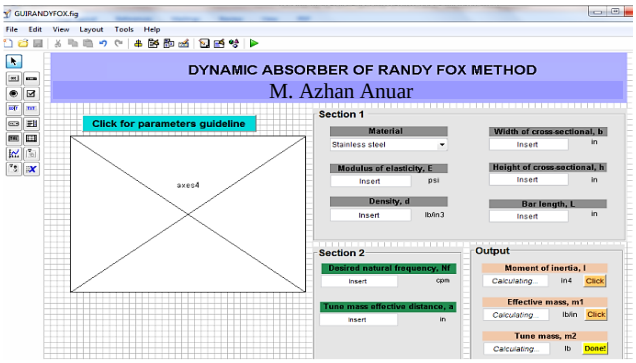

Figure-5. GUI template for Randy Fox method.

The Young's Modulus was experimentally calculated to ensure accuracy. A simple cantilever beam of the material used was setup and had its deflection measured before and after putting a known weight at its end which was solved using equation (12) as shown in Figure-6. The position of the tune mass is set at the end of the dynamic absorber, which is approximately at 0.2302 m from the clamping point.

$$E = \frac{PL^3}{3I\delta} \tag{12}$$

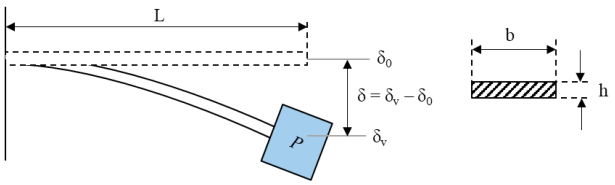

Figure-6. Calculation method for modulus of elasticity where δ_0 is the initial position, and δ_v is the final position after applying a load at the free end of the beam.

Experimental Setup and Measurement

The main system used was a vibration equipment setup as shown in Figure-7, consisting of a pin-connected beam attached with a spring. An imbalance exciter was placed at the centre to supply an excitation force to the system.

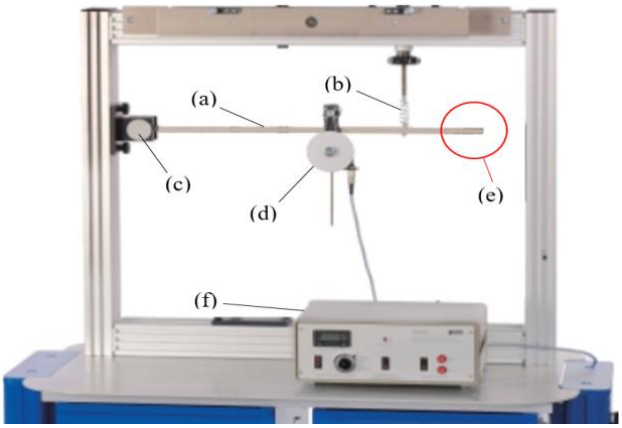

Figure-7. Gunt Hamburg TM 150 Vibration equipmentas the main system consisting of (a) rigid beam, (b) spring, (c) pinned-end support, (d) imbalance exciter, (e) DVA mounting location, and (e) control unit.

The dynamic absorber with piezoelectric was mounted on to the main system using a bolt, nut and washer as shown in Figure-8.

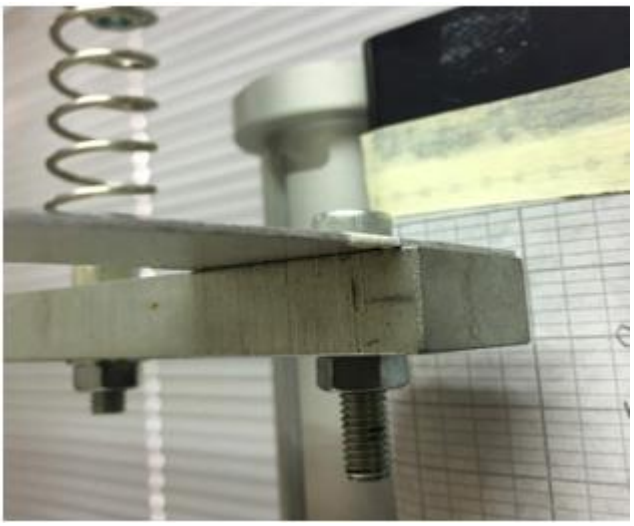

Figure-8. Close-up view on the dynamic absorber-main system mounting

Small plasticine was used as the tune mass for ease of adjustment and attachment on the absorber. The view of the camera was angled and directed such that the main system and DVA displaying their respective scales, imbalance control unit frequency's display screen and also the reading on the multi-meter. Deflection of the main system and tip of the DVA were measured throughout various range of frequencies. The experiment was repeated for DVA of different widths and the readings were recorded accordingly.

A Pro-Wave FS-2513P piezoelectric transducer was attached on the DVA closest to the bolting area using tape, where the highest strain is experienced for the fundamental mode shape of a cantilever beam vibration as shown in Figure-9.

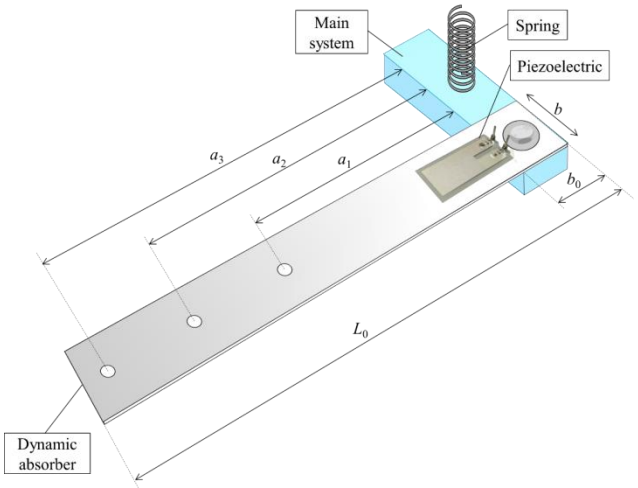

Figure-9. Illustration of setup and parameters for dynamic absorber design.

Displacement Measurement

The displacement of the main system and DVA were measured using high resolution, slow-motion camera at 240 frames per second. The video was compared to the scale plotted on the MDF board placed at the background of the view, showing both the main system and the DVA being measured. The complete arrangement of the experimental setup and the design parameters is illustrated in the following Figure-10. The response of the main system through frequency range of excitation was also measured to identify its natural frequency and displacement.

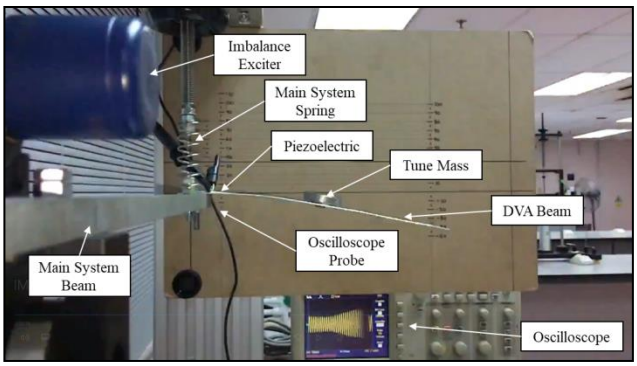

Figure-10. Experimental setup with DVA attached to the main system.

Energy Harvested from Voltage Generated

The piezoelectric pins were connected to a Tektronix TDS 2022B Oscilloscope using probe as depicted in Figure-11. The probe was connected to each of the two terminals on the piezoelectric to measure the generated peak voltage.

Figure-11. Tektronix TDS 2022B Oscilloscope and its probe

RESULTS AND DISCUSSIONS

The results of this study are presented in 4 aspects:

a) Displacement of main system without DVA.
b) Displacement of main system with DVA.
c) Displacement of DVA.
d) Voltage from piezoelectric transducer.

The displacement of the main system reflects the effectiveness of the DVA when the response was compared without and with the DVA. As for the displacement of the DVA, it reflects the strain experienced by the piezoelectric which is then expected to manifest in the voltage produced. For each aspect, all DVA designs were analysed with specific attention to the 3 frequencies of special interest as applicable:

a) At the original resonant frequency of the main system without DVA
b) At the first new resonant frequency of the system with the DVA
c) At the second new resonant frequency of the system with the DVA

Displacement of Main System without DVA

A frequency sweep was excited from 0 Hz to 12 Hz on the main system. The maximum peak was recorded at 9.1 Hz (546 cpm) with a displacement (i.e. amplitude) of 35 mm. It was identified that the targeted natural frequency of the original main system, ω_0, was as shown in Figure-12.

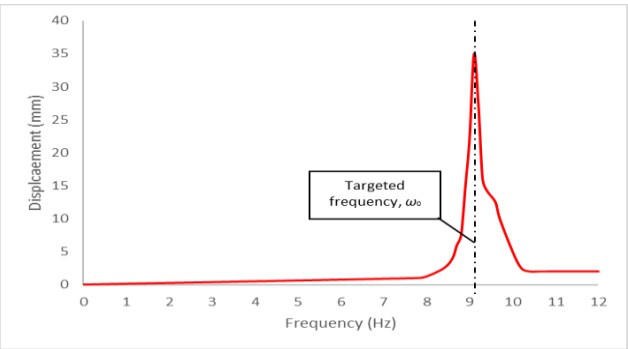

Figure-12. Displacement of main system without DVA against frequency.

Displacement of Main System with DVA

At the targeted frequency ω_0, the displacements for all designs were at the maximum of 2.5 mm as tabulated in Table-1 which indicate a significant reduction of amplitude by 92.5% of the original displacement without DVA.

Table-1. Displacement of main system at targeted frequency.

Tune Mass Position, a (mm)	Width of DVA, b (mm)	Targeted Frequency (Hz)	Displacement Amplitude (mm)
102	30	9.1	2.5
	40		1.7
	50		1.7
152	30	9.1	2.5
	40		1.7
	50		1.7
203	30	9.1	2.5
	40		1.7
	50		0.5

The first new resonant peak was noted at around 8.3 Hz to 8.5 Hz. For each tune mass position, the general trend shows that the first new resonant peak frequency decreases with an increase of width, *b*. The displacement (amplitude) on the other hand tends to decrease as the tune mass position moves farther away from the reference point as shown in Table-2.

Table-2. Displacement of main system at first new resonant peak.

Tune Mass Position, a (mm)	Width of DVA, b (mm)	First New Resonant Peak (Hz)	Displacement of Main System (mm)
102	30	8.5	20.0
	40	8.4	20.0
	50	8.3	20.0
152	30	8.5	17.5
	40	8.5	20.0
	50	8.3	17.5
203	30	8.5	10.0
	40	8.3	12.5
	50	8.3	12.5

The second new resonant peak does not clearly appear on the main system except when the tune mass position was at the farthest, 203 mm, which occured at around 9.9 Hz to 10.1 Hz with an amplitude of 5.0 mm.

The full data is plotted and shown in Figure-13 with additional main system without DVA where $b = 0$ for comparison purposes.

Displacement of DVA

At the targeted frequency ω_0, the displacement for all designs varied from a minimum of 5.0 mm to a maximum of 17.5 mm as shown in Table-3. The general trend shows the displacement (amplitude) increases as the tune mass position moves farther away from the reference point and as the DVA width becomes narrower.

Table-3. Displacement of DVA at targeted frequency.

Tune Mass Position, a (mm)	Width of DVA, b (mm)	Targeted Frequency (Hz)	Displacement of DVA (mm)
102	30	9.1	7.5
	40		7.5
	50		5.0
152	30	9.1	10.0
	40		10.0
	50		10.0
203	30	9.1	17.5
	40		15.0
	50		10.0

The first new resonant peak and general trend shows similar characteristics with the displacement of the main system. The first new resonant peak frequency appeared at the same frequencies, but the displacement amplitudes at the respective frequencies were manifolds larger than that of the main system as depicted in Table-4.

Table-4. Displacement of DVA at first new resonant peak.

Tune Mass Position, a (mm)	Width of DVA, b (mm)	First New Resonant Peak (Hz)	Displacement of DVA (mm)
102	30	8.5	65.0
	40	8.4	62.5
	50	8.3	62.5
152	30	8.5	67.5
	40	8.5	65.0
	50	8.3	65.0
203	30	8.5	75.0
	40	8.3	70.0
	50	8.3	65.0

In contrast to the displacement of the main system, the second new resonant peak for each design was clearly observed from the DVA displacement response, occurring around frequencies range from 9.9 Hz to 12.7 Hz as tabulated in Table-5. As the tune mass position moves farther away from the reference point, there were two trends can be clearly observed. The second new resonant frequency tends to appear closer to the targeted frequency while the displacement of the DVA tends to increase. The full data for DVA displacement is plotted and shown in Figure-14.

Table-5. Displacement of DVA at second new resonant peak.

Tune Mass Position, a (mm)	Width of DVA, b (mm)	Second New Resonant Peak (Hz)	Displacement of DVA (mm)
102	30	12.7	32.5
	40	12.6	40.0
	50	12.5	37.5
152	30	10.7	40.0
	40	11.2	42.5
	50	11.0	42.5
203	30	9.9	50.0
	40	10.1	50.0
	50	10.0	47.5

Voltage from Piezoelectric Transducer

As illustrated in Table-6, at the targeted frequency ω_0, the voltage for all designs varied from a minimum of 20.0 mV to a maximum of 40 mV. The general trend displays that the voltage increases as the tune mass position moves farther away from the reference point and as the DVA width becomes narrower.

Table-6. Peak voltage from Piezoelectric at targeted frequency.

Tune Mass Position, a (mm)	Width of DVA, b (mm)	Targeted Frequency (Hz)	Piezoelectric Peak Voltage (mV)
102	30	9.1	30.0
	40		30.0
	50		20.0
152	30	9.1	30.0
	40		30.0
	50		20.0
203	30	9.1	40.0
	40		40.0
	50		20.0

The first new resonant peak frequency appeared almost at all the same frequencies with the peaks observed from the displacements of the main system and the DVA. The trend of the voltage is not evidently clear with the change of tune mass position and width of DVA as shown in Table-7. However, the pattern of the trend discern similar trend to that of the displacement of the DVA, i.e. suggesting a proportional relationship.

Table-7. Peak Voltage from Piezoelectric at first new resonant peak.

Tune Mass Position, a (mm)	Width of DVA, b (mm)	First New Resonant Peak (Hz)	Piezoelectric Peak Voltage (mV)
102	30	8.5	150.0
	40	8.4	150.0
	50	8.3	110.0
152	30	8.5	210.0
	40	8.5	150.0
	50	8.3	110.0
203	30	8.5	175.0
	40	8.3	150.0
	50	8.3	90.0

Similar to the DVA displacement, the second new resonant peak for each design were clearly observed from the voltage response occurring around frequencies range of 9.9 Hz to 12.7 Hz as shown in Table-8, which is almost exactly the same as that from DVA displacement. As the tune mass position moves farther away from the reference point, the second new resonant frequency tends to appear closer to the targeted frequency similar to that of the DVA displacement. Despite the inconclusive voltage relationship for various tune mass position and width of DVA, the pattern shows similar characteristics with that of the DVA displacement, indicating a proportional relationship. The full data for peak voltage against frequency is plotted in Figure-15.

Table-8. Peak voltage from Piezoelectric at second new resonant peak.

Tune Mass Position, a (mm)	Width of DVA, b (mm)	Second New Resonant Peak (Hz)	Piezoelectric Peak Voltage (mV)
102	30	12.7	150.0
	40	12.6	175.0
	50	12.5	130.0
152	30	10.7	150.0
	40	11.2	160.0
	50	11.0	120.0
203	30	9.9	150.0
	40	10.0	200.0
	50	10.0	130.0

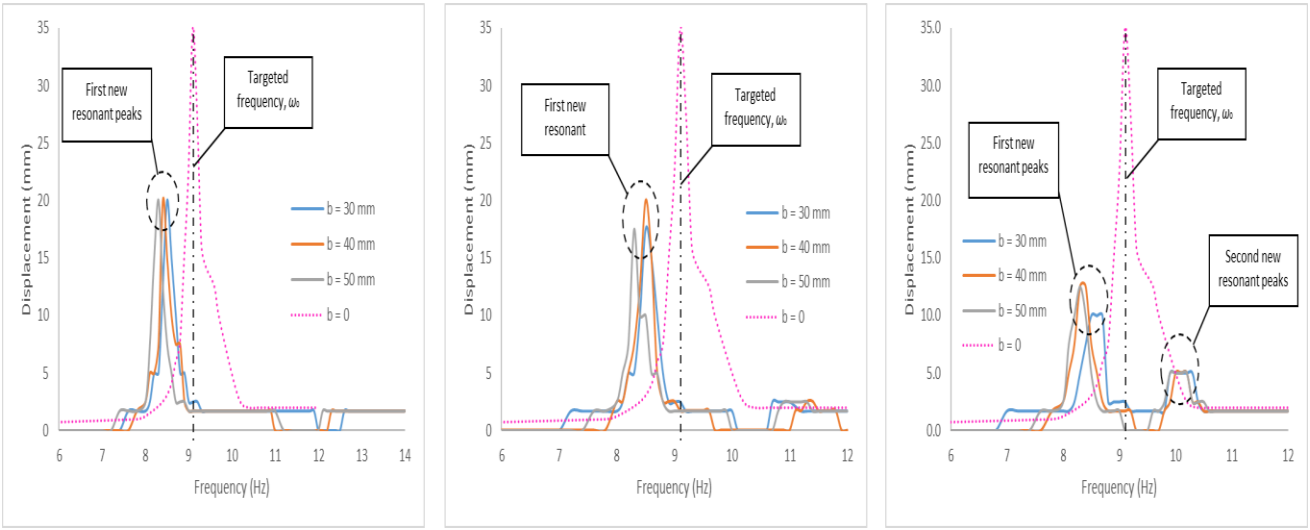

Figure-13. Displacement of main system without DVA and with DVA against frequency with a = 102 mm (left), a = 152 mm (center), and a = 203 mm (right).

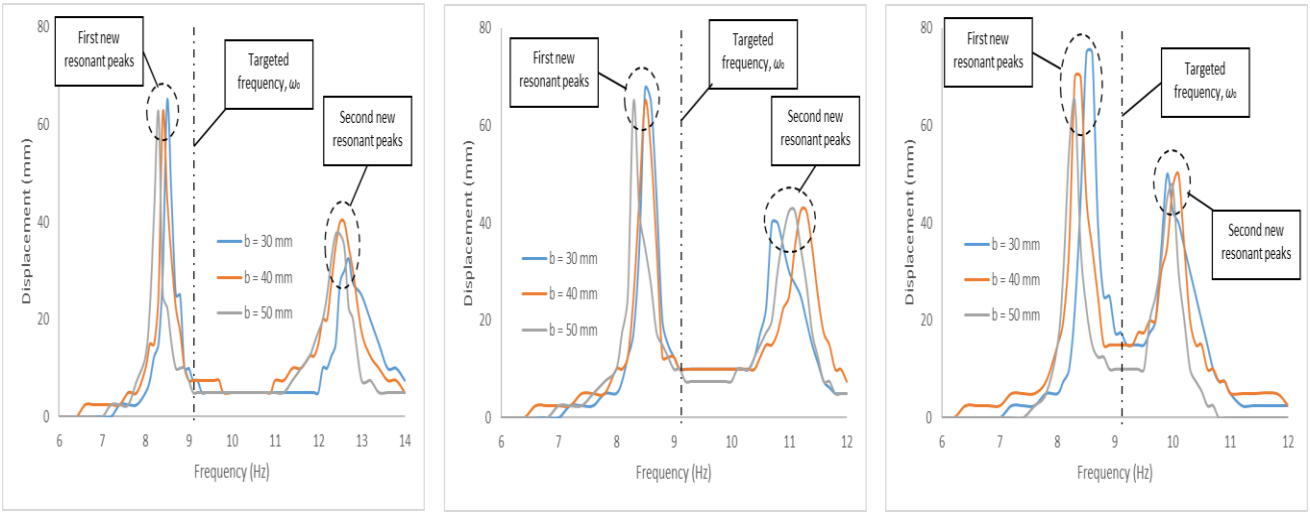

Figure-14. Displacement of DVA against frequency with a = 102 mm (left), a = 152 mm (center), and a = 203 mm (right).

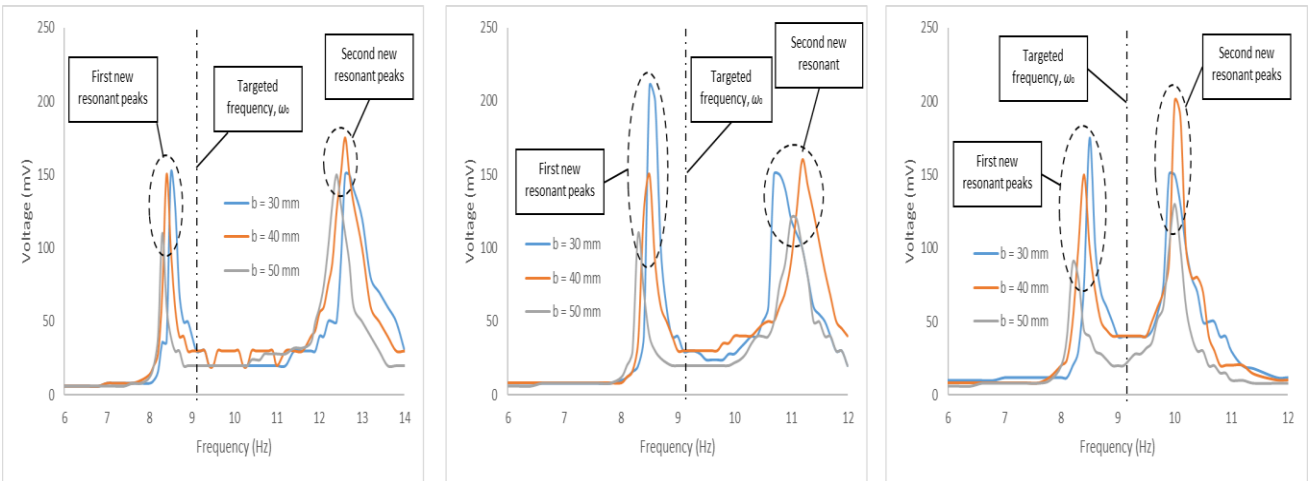

Figure-15. Peak voltage from piezoelectric transducer against frequency with a = 102 mm (left), a = 152 mm (center), and a = 203 mm (right).

CONCLUSIONS

The study found that at the targeted frequency, the vibration of the main system is effectively attenuated by the DVA for all designs. For energy harvesting, the best DVA should have the farthest tune mass position from its reference point, *a* and the narrowest width of the DVA, *b*. It can be concluded from the relationships that the peak voltage is proportional to DVA displacement, and the DVA displacement is proportional to the tune mass position and inversely proportional to the width of the DVA.

A second new resonant peak begins to appear on the main system as the tune mass position increases. Hence, in the design process, this must be considered in case there is excitation frequency in the range of these new frequencies. If this occurs, the DVA should be redesigned to ensure that the frequencies are farther away from the excitation frequency.

This study indicates that the application of DVA as energy harvesting system using RFM is effective in reducing the vibration of the main system as hypothesized. It is recommended that the research be extended to investigate the effectiveness of the DVA design to generate more energy using other methods such as Rayleigh and Dunkerley. In addition, a better transducer than piezoelectric materials and its electrical elements for better energy harvest and storage could be used to ensure that the system perform more effectively.

REFERENCE

[1] T. Lauwagie, R. Van Assche, J. Van der Straeten and W. Heylen. 2006. A Comparison of Experimental, Operational, and Combined Experimental-Operational Parameter Estimation Techniques. in Proceedings of the International Noise and Vibration Conference, ISMA 2006.

[2] M. M. Salleh, I. Zaman and A. L. M. Tobi. 2016. Modification of vibrating thin walled structure using dynamic vibration absorber. ARPN J. Eng. Appl. Sci.

[3] T. V. V. L. N. Rao, A. A. Mokhtar, M. Muhammad, and P. Hussain. 2016. Optimally tuned active damped dynamic vibration absorber. ARPN J. Eng. Appl. Sci.

[4] L. Liu and W. Shao. 2011. Design and Dynamic Response Analysis of Rail with Constrained Damped Dynamic Vibration Absorber. Procedia Eng. 15: 4983-4987.

[5] X. Huang, Z. Su and H. Hua. 2018. Application of a dynamic vibration absorber with negative stiffness for control of a marine shafting system. Ocean Eng.

[6] Y. Khazanov. 2007. Dynamic Vibration Absorbers - Application with Variable Speed Machines.

[7] N. Debnath, A. Dutta and S. K. Deb. 2016. Multi-modal Passive-vibration Control of Bridges under General Loading-condition. Procedia Eng. 144: 264-273.

[8] O. Fischer. 2007. Wind-excited vibrations-Solution by passive dynamic vibration absorbers of different types. J. Wind Eng. Ind. Aerodyn. 95(9-11): 1028-1039.

[9] H. E. Tseng and D. Hrovat. 2015. State of the art survey: Active and semi-active suspension control. Veh. Syst. Dyn.

[10] M. A. Anuar, A. A. M. Isa, A. R. Zamri and R. Brincker. 2018. Critical experimental issues of cracked aluminum beam in operational modal analysis. J. Mech. Eng. 5(Special issue 6): 211-225.

[11] M. A. Anuar, S. A. Samat and A. A. Mat Isa. 2017. Experimental analysis to evaluate the effect of Dynamic Absorber. J. Mech. Eng. SI 4(4): 242-262.

[12] Richard Smith (Beloit Corporation). 1998. Dynamic Vibration Absorbers. S V Sound Vib. 32(11): 24-27.

[13] S. A. Samat, A. A. Mat Isa and M. A. Anuar. 2017. Performance evaluation of Dynamic Absorbers based on randy fox and Dunkerley Methods. J. Mech. Eng. SI 4(4): 263-279.

[14] S. F. Ali and S. Adhikari. 2013. Energy harvesting dynamic vibration absorbers. J. Appl. Mech. Trans. ASME.

[15] Y. J. Wang, T. Y. Chuang and C. Lee. 2019. Resonant frequency self-tunable piezoelectric cantilevers for energy harvesting and disturbing torque absorbing. Sensors Actuators, A Phys.

[16] J. Wang, Z. Shi, H. Xiang and G. Song. 2015. Modeling on energy harvesting from a railway system using piezoelectric transducers. Smart Mater. Struct.

[17] T. Nayyar, K. Pubby, S. B. Narang and R. Mishra. 2016. Energy harvesting using piezoelectric materials. Integr. Ferroelectr.

[18] N. Jalili. 2010. Piezoelectric-based vibration control: From macro to micro/nano scale systems.

[19] C. Y. Lee and J. H. Lin. 2017. Incorporating piezoelectric energy harvester in tunable vibration absorber for application in multi-modal vibration reduction of a platform structure. J. Sound Vib.

[20] R. Fox. Dynamic Absorbers for Solving Resonance Problems. Entek IRD International Corp, Houston. pp. 1-14.